The Astrophysical Journal, 708:L18–L21, 2010 January 1 doi:10.1088/2041-8205/708/1/L18

ATOMIC CARBON IN THE UPPER ATMOSPHERE OF TITAN

X. Zhang[1], J. M. Ajello[2], and Y. L. Yung[1]
[1] Division of Geological and Planetary Sciences, California Institute of Technology, Pasadena, CA, 91125, USA
[2] Jet Propulsion Laboratory, California Institute of Technology, Pasadena, CA 91109, USA
Received 2009 September 28; accepted 2009 November 25; published 2009 December 11

ABSTRACT

The atomic carbon emission C I line feature at 1657 Å ($^3P_J^0$–^3P_J) in the upper atmosphere of Titan is first identified from the airglow spectra obtained by the Cassini Ultra-violet Imaging Spectrograph. A one-dimensional photochemical model of Titan is used to study the photochemistry of atomic carbon on Titan. Reaction between CH and atomic hydrogen is the major source of atomic carbon, and reactions with hydrocarbons (C_2H_2 and C_2H_4) are the most important loss processes. Resonance scattering of sunlight by atomic carbon is the dominant emission mechanism. The emission intensity calculations based on model results show good agreement with the observations.

Key words: planets and satellites: individual (Titan) – radiative transfer – scattering

Online-only material: color figures

1. INTRODUCTION

Titan's airglow spectra measured by the Ultra-violet Imaging Spectrograph (UVIS) on Cassini on 2004 December 13 provide the first detection of atomic carbon emission features in Titan's upper atmosphere (Ajello et al. 2008; Gustin et al. 2009). One of the strongest carbon C I line emissions is identified, corresponding to the resonance multiplets of neutral atomic carbon at 1657 Å ($^3P_J^0$–^3P_J). The signal of the other C I line (1561 Å ($^3D_J^o$–^3P_J)) is below the noise level because its line intensity is weaker. This observation provides an opportunity to study atomic carbon in the upper atmosphere of Titan. In this Letter, first we use the Caltech/JPL one-dimensional photochemical model (Yung et al. 1984; Moses et al. 2000, 2005; Liang et al. 2007) to simulate the concentration and distribution of atomic carbon, and discuss its major sources and sinks. We then calculate the limb emission intensities based on the model results for the two C I lines and compare the 1657 Å line intensities to the observation. This is followed by comparisons with previous studies of carbon atoms in the atmosphere of Mars and Venus (e.g., McElroy & McConnell 1971; Fox 1982) and a discussion of the implications of the model on the chemistry for Titan.

2. PHOTOCHEMICAL MODEL

It is difficult for photons or electrons to dissociate CH_4 and produce atomic carbon, because of the high binding energy of the C–H bond in the CH_4 molecule (Pang et al. 1987). Breaking all four C–H bonds per mole of CH_4 requires 1662 kJ. Indeed, the main production mechanism of atomic carbon on Titan is via the production of the CH radical in a chain of chemical reactions initialized by the photolysis of CH_4 by sunlight with wavelengths shorter than 1600 Å (Yung et al. 1984). Figure 1 illustrates the important reaction pathways for producing and destroying atomic carbon and related hydrocarbons in the upper atmosphere of Titan.

The concentration profile of atomic carbon in the upper atmosphere of Titan is simulated by the Caltech/JPL kinetics one-dimensional photochemical model (Yung & Allen 1984; Moses et al. 2000, 2005). In this model, we took into account species including the most abundant hydrocarbons and nitriles and solved the mass continuity equation above the tropopause (∼50 km):

$$\frac{\partial n_i}{\partial t} + \frac{\partial \varphi_i}{\partial z} = P_i - L_i, \quad (1)$$

where n_i is the number density for species i, φ_i is the vertical flux, P_i is the chemical production rate, and L_i is the chemical loss rate, all evaluated at time t and altitude z. The vertical flux is given by

$$\varphi_i = -\frac{\partial n_i}{\partial z}(D_i + K_{zz}) - n_i\left(\frac{D_i}{H_i} + \frac{K_{zz}}{H_a}\right) - n_i\frac{\partial T}{\partial z} \times \left[\frac{(1+\alpha_i)D_i + K_{zz}}{T}\right], \quad (2)$$

where K_{zz} is the eddy diffusion coefficient, D_i is the molecular diffusion coefficient, H_i is the scale height for species i, H_a is the atmospheric scale height, α_i is the thermal diffusion parameter, and T is the temperature.

The photochemical reactions are taken from the list in Moses et al. (2005). In Table 1, we summarize the important production and loss processes of atomic carbon and the corresponding integrated column reaction rates in our model. The reaction numbers are exactly the same as those in Moses et al. (2005) except for the CH photolysis reaction (R164). Therefore, all the reaction rate constants and related references (except R164) can be found in the auxiliary material Table S3 of that paper. The cross sections of CH photo-dissociation (R164) are obtained from van Dishoeck (1988).

The mixing ratio of CH_4 in the deep atmosphere is prescribed to be 2.275×10^{-2} (Liang et al. 2007), and we fixed the atomic hydrogen and molecular hydrogen escape velocities in the top atmosphere as 2.5×10^4 cm s^{-1} and 6.1×10^3 cm s^{-1}, respectively. All species except hydrogen and carbon monoxide will leave the lower boundary with the velocity 2×10^{-4} cm s^{-1}, due to the cold trap at the tropopause. The atmospheric temperature profile is based on the Cassini measurements (Liang et al. 2007). The eddy diffusion coefficient profile is constrained by recent Cassini UVIS stellar occultation data (D. E. Shemansky 2009, private communication). Above the homopause (around 1000 km), the molecular diffusion process dominates.

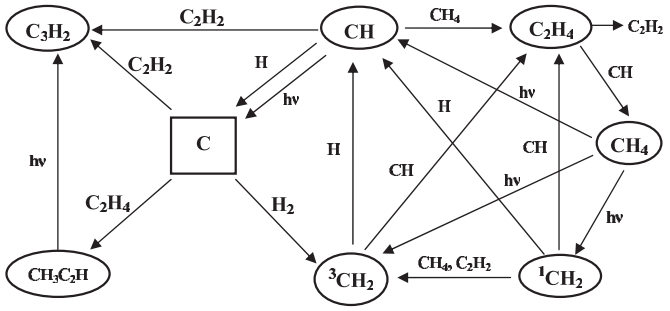

Figure 1. Schematic diagram illustrating the important reaction pathways related to atomic carbon.

Table 1
Important Reactions Involving Atomic Carbon

Reaction	Integrate Column Reaction Rate[a]
Sources	
(R182) $H + CH \rightarrow C + H_2$	2.014×10^7
(R164) $CH \rightarrow C + H$	1.078×10^5
Sinks	
(R238) $C + H_2 \xrightarrow{M} {}^3CH_2$	1.003×10^7
(R239) $C + C_2H_2 \xrightarrow{M} C_3H_2$	9.634×10^6
(R240) $C + C_2H_4 \xrightarrow{M} CH_3C_2H$	5.819×10^5

Notes. The reaction numbers are the same as those in Moses et al. (2005) except the R164. All the reaction rate constants and related references (except R164) can be found in the auxiliary material Table S3 of that paper. The cross sections of CH photodissociation (R164) are obtained from van Dishoeck (1988).
[a] Integrated column reaction rate is in units of cm^{-2} s^{-1}.

More than 80% of CH radicals are removed by reacting with CH_4 to form C_2H_4, but a small portion of CH (less than 1% in the upper atmosphere) react with atomic hydrogen to produce carbon atoms (R182 in Table 1):

$$H + CH \rightarrow C + H_2.$$

Atomic carbon can also be produced by the CH photodissociation (R164), but the production rate is negligible compared with the R182 (see the discussion below). The major loss of atomic carbon is through the reaction with molecular hydrogen to form CH_2 (R238) in the lower atmosphere. In the upper atmosphere, the dominant sinks of atomic carbon are the reactions with hydrocarbons like C_2H_2 (R239) and C_2H_4 (R240) to produce C_3 hydrocarbons.

The concentration profiles of atomic carbon together with CH, CH_4, and atomic hydrogen above 400 km are shown in the left panel of Figure 2. Two CH_4 observation data points from Niemann et al. (2005) and Waite et al. (2005) are also shown in the figure. The plot shows that our model results match the measurements very well. The CH abundance is roughly 100 molecules cm^{-3} at its peak around 1250 km. Our model results are in general agreement with recent models of Titan (Dobrijevic et al. 2008; Krasnopolsky 2009). The similar pattern of the H and C concentration profiles suggests that the production of C is directly correlated with abundance of H (R182), not only because H is one of the reactants, but also because the atomic hydrogen is directly involved in the production processes of CH (Figure 1).

The right panel of Figure 2 shows the production and loss rates involved in the photochemistry of atomic carbon. The production rate of R164 is two orders of magnitude less than

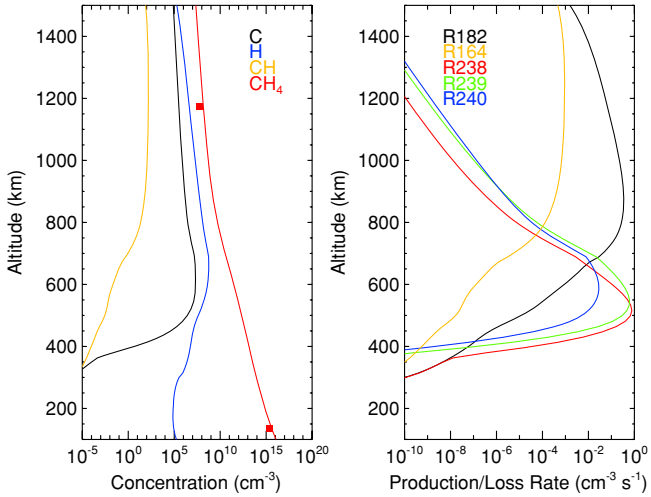

Figure 2. Left panel: concentration profiles of atomic carbon, CH, CH_4, and atomic hydrogen (labeled by colors). Two CH_4 observation data points from Niemann et al. (2005) and Waite et al. (2005) are shown by filled squares. Right panel: production rate (R182 and R164) and loss rate (R238, R239, and R240) of atomic carbon due to the most important four reactions (labeled by colors).
(A color version of this figure is available in the online journal.)

that of R182 at 1200 km. Therefore, the CH+H reaction (R182) is the dominant source of atomic carbon. The loss rate curves display clearly that in the lower atmosphere of Titan, the reaction with H_2 is the major loss process of C (R238). However, in the upper atmosphere (above 800 km), C_2H_2 and C_2H_4 dominate the loss of C (R239 and R240). At 1200 km, the contribution of R239 to the loss rate is about 34% and that of R240 is about 61%.

The contribution of nitrogen chemistry to the C production is negligible. The main sources of C in nitrogen chemistry are the photolysis of CN and the reaction between N atom and CN, which is analogous to R182:

$$N + CN \rightarrow C + N_2.$$

In our model, the abundances of CN and N are about 1×10^3 cm^{-3} and 1×10^5 cm^{-3} in the upper atmosphere. The photolysis rate of CN above 1000 km is around 3×10^{-8} s^{-1}. Therefore, the C production rate is on the order of 10^{-5} cm^{-3} s^{-1} due to CN photodissociation. The rate coefficient for the reaction between N and CN, according to Atakan & Wolfrum (1992), is 3.24×10^{-13} $e^{(-1771/T)}$ between 298 K and 534 K. In the upper atmosphere of Titan, the rate should be even smaller because the temperature is cooler than 150 K. Actually, the production rate of C due to this reaction is around 10^{-10} cm^{-3} s^{-1} above 1000 km. Both of these two production rates are negligible compared with the production rate from R182, which is on the order of 10^{-2} cm^{-3} s^{-1} based on the reaction rate coefficient from van Harrevelt et al. (2002).

Given the main sources and sinks of atomic carbon, the steady-state concentration of which can be expressed as (the diffusion term is ignored because the chemical reaction timescale is short)

$$\frac{[C]}{[CH]} = \frac{J_{164} + k_{182}[H]}{k_{238}[H][M] + k_{239}[C_2H_2][M] + k_{240}[C_2H_4][M]}, \quad (3)$$

where M is the bath gas and J_{164} refers to the photolysis rate coefficient. k_{182}, k_{238}, k_{239}, and k_{240} are the reaction rate coefficients for R182, R238, R239, and R240, respectively. The

Table 2
Atomic Data for the Transitions of the Mulitplets 2 and 3 in C I

Transition	λ (Å)	$f(10^{-2})$
$2p^2\ 3P–3s\ ^3P^\circ$		
$^3P_1–^3P_2$	1656.2672	5.89
$^3P_0–^3P_1$	1656.9283	13.9
$^3P_2–^3P_2$	1657.0082	10.4
$^3P_1–^3P_1$	1657.3792	3.56
$^3P_1–^3P_0$	1657.9068	4.73
$^3P_2–^3P_1$	1658.1212	3.56
$2p^2\ 3P–2p\ ^3\ ^3D^\circ$		
$^3P_0–^3D_1$	1560.3092	7.19
$^3P_1–^3D_2$	1560.6822	5.39
$^3P_1–^3D_1$	1560.7090	1.80
$^3P_2–^3D_2$	1561.3402	1.08
$^3P_2–^3D_1$	1561.3667	0.07
$^3P_2–^3D_3$	1561.4384	6.03

concentration of CH is nearly independent of C because most of the CH radicals are destroyed by reacting with CH_4 in the high altitude. A full set of photochemical reactions (more than 900 reactions) is used to model the concentrations of all the hydrocarbon species and gives robust results for C_2H_2, C_2H_4, CH, and H. The main uncertainty is due to the reaction R182. From Equation (3), because J_{164} can be neglected compared with the reaction rate of CH+H, the concentration of atomic carbon is proportional to the rate coefficient k_{182}. For example, in our study, we use the reaction rate coefficient from van Harrevelt et al. (2002) and the atomic carbon density is 2.7×10^7 cm^{-3} at 1200 km. This value is 30% larger than the carbon abundance (2.0×10^7 cm$^{-3)}$ calculated based on the rate coefficient from Harding et al. (1993). The ratio of the two rate coefficients under the temperature at 1200 km is roughly 1.3. However, our radiative modeling study (Section 3) shows that the limb emission spectrum is not very sensitive to the 30% concentration difference.

3. CARBON EMISSIONS

Previous studies suggest that the resonance scattering of sunlight by atomic carbon contributes the most to the observed intensities at 1561 Å and 1657 Å (e.g., McElroy & McConnell 1971). In order to compare our photochemical model results with observed airglow data, we computed the resonant scattering emission intensities of the carbon C I lines at 1561 Å and 1657 Å by a pseudo-spherical radiative transfer method. First we assume a local plane parallel layering atmosphere. Based on the one-dimensional photochemical model results, the source function for each layer is computed from a multiple scattering calculation by the DISORT model (Stamnes et al. 1988). The limb radiance can be obtained by solving the radiative transfer equation along the line of sight.

For each transition line, the absorption coefficient per atom at rest can be expressed as $\frac{\pi e^2}{mc} f$, where f is the oscillator strength and $\pi e^2/mc$ (=2.647×10^{-2} cm^2 s^{-1}) is the integrated absorption coefficient per atom for unit f-value, and e and m are the charge and mass of an electron, respectively. The atomic data for the transitions of the mulitplets 2 and 3 in C I are shown in Table 2. The f-values and vacuum wavelengths are obtained from Wiese et al. (1996) and Morton (1991), respectively. When the carbon atoms are in thermal motion, the absorption line shape follows a Voigt profile, which is the convolution of the Lorentz and Doppler (Gaussian) line shapes. The pressure broadening effect is negligible in the upper atmosphere of Titan. Therefore, the Doppler line profile is dominant, and the FWHM of each line is roughly proportional to the square root of the atmospheric temperature, on the order of several mÅ. The single scattering albedo of atomic carbon is approximately unity because in the upper atmosphere of Titan, the optical depth of atomic carbon is about 1–10 (at the line center), whereas the optical depth from all of the other gas species is only on the order of 10^{-3} and the contribution from the tholin is roughly 10^{-2} based on the tholin profile from Liang et al. (2007). We took solar C I emission spectra on 2004 December 13 from the Composite Solar Ultraviolet Spectral Irradiance Data Set (Deland & Cebula 2008), which provide the daily average solar spectra over the wavelength range 120–400 nm in 1 nm bins from 1978 November 8 to 2005 August 1.

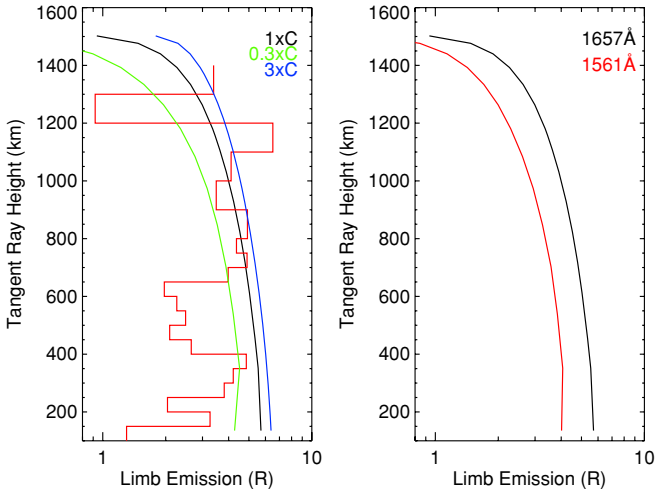

Figure 3. Left panel: modeled limb intensities for 1657 Å, compared with Cassini limb observational data (red line). The intensities are in units of Rayleigh (1 Rayleigh (R) = 10^6 photons cm^{-2} s^{-1}). A sensitivity study has been made for 0.3 times and 3 times the carbon abundances from the photochemical model results. Right panel: modeled limb intensities for 1657 Å (black line) and 1561 Å (red line).

(A color version of this figure is available in the online journal.)

The limb intensities of resonance scattering emissions are shown in Figure 3. The left panel shows the modeled limb emissions at 1657 Å for each tangent ray height and compared with the observed data (in red). The measured intensities are determined by differencing in 50 and 100 km increments the intensities of the UVIS limb airglow spectral feature at 1657 Å (within the 5.5 Å FWHM bandpass) with the composite airglow model: a sum of (1) reflected sunlight from Rayleigh scattering and (2) Lyman–Birge–Hopfield (LBH) band system and N I multiplet airglow emissions (Ajello et al. 2008).

Our photochemical model results agree with the Cassini data above 600 km. The left panel of Figure 3 also illustrates the sensitivity of the carbon abundances to the modeled emission intensities. Since the upper atmosphere is optically thick due to strong carbon absorption, the change of carbon number density by a factor of 3 results in a change of emission intensity by only 20%–50%, approximately. We attribute the discrepancy between the model and data to the error associated in subtracting the large contribution of reflected sunlight at 1657 Å (Ajello et al. 2008). The predicted limb emission of 1561 Å is shown in the right panel. The limb emission profiles for the two lines are very similar. The magnitude at 1561 Å is only 30% of that at 1657 Å although the total line intensity at 1561 Å is about half

of that at 1657 Å. The reason is that the emission efficiency is reduced by the optically thick upper atmosphere.

4. DISCUSSION AND CONCLUSIONS

The carbon atoms have been observed on Mars and Venus. The photochemistry of atomic carbon in the upper atmosphere of Mars was first studied by McElroy & McConnell (1971) based on the Mars-Mariner emission spectra (Barth et al. 1971). They also discussed the abundance and profile of atomic carbon in the upper atmosphere of Venus, but no spectral data were available until the Pioneer Venus Orbiter measurements (Stewart et al. 1979; Niemann et al. 1980; Taylor et al. 1980). Based on these data, Fox (1982) and Paxton (1985) used photochemical models to investigate the reactions of atomic carbon and possible emission mechanisms on Venus. Both of the two previous studies show that the production mechanisms of atomic carbon on Mars and Venus are photodissociation and electron-impact dissociation of CO_2 and CO, and the primary sink of C is the reaction with O_2, along with some contribution from the reaction with NO. Fox (2004) and Fox & Paxton (2005) revisited the photochemistry of atomic carbon for Mars and Venus, respectively. Fox (2004) discovered that dissociative recombination CO_2^+ is the most important source of atomic carbon in the Martian thermosphere. Fox & Paxton (2005) confirmed that the CO photodissociation is the dominant production process of atomic carbon on Venus.

By contrast, in a non-oxidizing environment such as Titan, the photochemistry of atomic carbon is quite different. As a natural laboratory of hydrocarbon chemistry, Titan starts its photochemistry from the photolysis of CH_4. Atomic carbon only plays a minor role in one small branch of the complex network of all known hydrocarbon reactions (Figure 9 in Moses et al. 2005). Our study suggests that the nitrogen chemistry contributes little to the production of C. Atomic hydrogen is a key reactant in producing atomic carbon, and the C_2 hydrocarbons like C_2H_2 and C_2H_4 above 600 km dominate the loss processes. Compared with Venus and Mars, the photochemistry of C in Titan's upper atmosphere is relatively simple because there is no direct source from photon- or electron-induced dissociation. However, since C is related to several of the most important species, for example, CH_4, CH, H, C_2H_2, and C_2H_4, a full set of photochemical reactions (at least the C_3 chemistry) needs to be taken into account. Based on the current knowledge of photochemistry and transport processes on Titan, our one-dimensional photochemical model is able to produce an atomic carbon vertical profile, based on which we can reproduce the Cassini limb observation at 1657 Å by simple resonant scattering calculation. This agreement confirms previous results in other planets that the observed intensities at 1561 Å and 1657 Å arise mostly from the resonance scattering of sunlight by atomic carbon, and shows that our knowledge of the photochemical behavior of C in Titan's upper atmosphere is roughly complete. We also predict the 1561 Å limb emission intensity, which remains to be confirmed by future observations.

We thank M. C. Liang and J. I. Moses for making their updated kinetics for the Titan model available and D. E. Shemansky for providing the Cassini UVIS stellar occultation data, V. Natraj, M. Line, and M. Gerstell for reading the manuscript. We thank an anonymous referee for providing updates of reaction coefficients. The research was supported in part by NASA PATM grant NNX09AB72G to the California Institute of Technology.

REFERENCES

Ajello, J. M., et al. 2008, Geophys. Res. Lett., 35, L06102
Atakan, B., & Wolfrum, J. 1992, Chem. Phys. Lett., 186, 547
Barth, C. A., Hord, C. W., Pearce, J. B., Kelly, K. K., Anderson, G. P., & Stewart, A. I. 1971, J. Geophys. Res., 76, 2213
Deland, M. T., & Cebula, R. P. 2008, J. Geophys. Res., 113, A11103
Dobrijevic, M., Carrasco, N., Hébrard, E., & Pernot, P. 2008, Planet. Space Sci., 56, 1630
Fox, J. L. 1982, J. Geophys. Res., 87, 9211
Fox, J. L. 2004, J. Geophys. Res., 109, A08306
Fox, J. L., & Paxton, L. J. 2005, J. Geophys. Res., 110, A01311
Gustin, J., Ajello, J. M., Stevens, M. H., Stepfan, A. W., Stewart, I., Larsen, K., Esposito, L., & McClintock, W. 2009, Geophys. Res. Lett.,, submitted
Harding, L. B., Guadagnini, R., & Schatz, G. C. 1993, J. Phys. Chem., 97, 5472
Krasnopolsky, V. A. 2009, Icarus, 201, 226
Liang, M., Yung, Y. L., & Shemansky, D. E. 2007, ApJ, 661, L199
McElroy, M. B., & McConnell, J. C. 1971, J. Geophys. Res., 76, 6674
Morton, D. C. 1991, ApJS, 77, 119
Moses, J. I., Bezard, B., Lellouch, E., Gladstone, G. R., Feuchtgruber, H., & Allen, M. 2000, Icarus, 143, 244
Moses, J. I., Fouchet, T., Bézard, B., Gladstone, G. R., Lellouch, E., & Feuchtgruber, H. 2005, J. Geophys. Res., 110, E08001
Niemann, H. B., Kasprzak, W. T., Hedin, A. E., Hunten, D. M., & Spencer, N. W. 1980, J. Geophys. Res., 85, 7817
Niemann, H. B., et al. 2005, Nature, 438, 779
Pang, K. D., Ajello, J. M., Franklin, B., & Shemansky, D. E. 1987, J. Chem. Phys., 86, 2750
Paxton, L. J. 1985, J. Geophys. Res., 90, 5089
Stamnes, K., Tsay, S.-C., Jayaweera, K., & Wiscombe, W. 1988, Appl. Opt., 27, 2502
Stewart, A. I., Anderson, D. E., Esposito, L. W., & Barth, C. A. 1979, Science, 203, 777
Taylor, H. A., Brinton, H. C., Bauer, S. J., Hartle, R. E., Cloutier, P. A., & Daniell, R. E. 1980, J. Geophys. Res., 85, 7765
van Dishoeck, E. F. 1988, in Rate Coefficients in Astrochemistry, ed. T. J. Millar & D. A. Williams (Dordrecht: Kluwer), 49
van Harrevelt, R., van Hemert, M. C., & Schatz, G. C. 2002, J. Chem. Phys., 116, 6002
Waite, J. H., Jr., et al. 2005, Science, 308, 982
Wiese, W. L., Fuhr, J. R., & Deters, T. M. (ed.) 1996, in J. Phys. Chem. Ref. Data, Mono., Vol. 7, Atomic Transition Probabilities of Carbon, Nitrogen, and Oxygen: A Critical Data Compilation (Washington, DC: American Chemical Society)
Yung, Y. L., Allen, M., & Pinto, J. P. 1984, ApJS, 55, 465